Kinetic Studies of Anthracycline–DNA Interaction by Fluorescence Stopped Flow Confirm a Complex Association Mechanism

Vincenzo Rizzo,* Nereo Sacchi, and Milena Menozzi
Research and Development, Farmitalia Carlo Erba, Via dei Gracchi 35, I-20146 Milano, Italy
Received April 6, 1988; Revised Manuscript Received July 21, 1988

ABSTRACT: The kinetics of association and dissociation between calf thymus DNA and five anthracyclines, including doxorubicin, daunorubicin, and three synthetic analogues, were investigated with stopped flow using fluorescence detection. The sensitivity of this technique allowed us to work with submicromolar drug concentrations, thus excluding formation of aggregates, and with ratios of DNA base pairs to drug in the range 10–250, where site exclusion effects could be taken into account with a simple correction of DNA concentration and pseudo-first-order conditions were nearly fulfilled. In all cases, both association and dissociation reactions required a sum of three exponential terms to be fitted. However, satisfactory interpretation of reciprocal relaxation times as functions of DNA concentration was only achieved with kinetic models comprising a total of five steps. One of the extra steps was tentatively assigned to formation of a weakly bound, probably nonintercalated species. Another step was deduced from a comparison between results of association and dissociation experiments. The five steps are arranged, for convenience, in an association mechanism with two branches, though other mechanisms cannot be definitely ruled out. Correlation of cytotoxicity data with both association and dissociation rates is not found to be significant. This suggests that other factors must be involved in modulating the different biological properties of the investigated anthracyclines.

Anthracyclines are a class of antibiotics produced by several *Streptomyces* species and comprising powerful and widely used antitumor drugs such as daunorubicin (**1**, daunomycin) and doxorubicin (**2**, adriamycin). The cytotoxic activity of these compounds is thought to be mediated by their interaction with DNA (Arcamone, 1981). An intercalative mode of interaction with DNA is strongly supported from studies in solution [for a review, see Fritzsche and Berg (1987)] and from crystallographic analysis of a complex between daunorubicin and an oligonucleotide (Quigley et al., 1980; Wang et al., 1987). Less well characterized is the kinetic mechanism of interaction, although the importance of dissociation rates on the biological effects of intercalators has been pointed out in a classical work by Mueller and Crothers (1968). Moreover, a correlation between transcription inhibition and dissociation rate of DNA complexes has been reported (Phillips & Crothers, 1986) for a group of intercalators including daunorubicin (**2**), and more recently, a correlation has been suggested between the on-rate of drug–DNA interaction and disruption of the open complex between RNA polymerase and DNA (Straney & Crothers, 1987).

Multiexponential behavior has been reported for association/dissociation kinetics of **1** and **2** with DNA (Foerster & Stutter, 1984; Chaires et al., 1985; Fox et al., 1985; Krishnamoorthy et al., 1986). Site exclusion may in part explain such complexity (Epstein, 1979), because about three base pairs are involved in daunorubicin binding (Wang et al., 1987). On the other hand, a multistep intercalation mechanism may be involved, as observed with actinomycin (Mueller & Crothers, 1968) and proposed for simple intercalators such as tilorone (Sturm, 1982). Temperature jump relaxation kinetics carried out on DNA complexes of **1** and **2** at low nucleotide/drug ratio have been interpreted in terms of site exclusion effects with a simple one-step association process (Foerster & Stutter, 1984). Alternatively, a three-step association mechanism has been proposed in a study of daunorubicin–DNA interaction carried out with stopped flow using absorption detection (Chaires et al., 1985) at higher nucleotide/drug ratios. Confirming this latter result is interesting because such a multistep mechanism may be interpreted as evidence of binding site heterogeneity (Sturm, 1982). In fact, the nature and even the existence of sequence specificity in anthracycline–DNA binding have been controversial (Neidle & Abraham, 1984), and only recent theoretical (Chen et al., 1985) and experimental (Chaires et al., 1987) investigations consistently indicated preferential binding sites made of two adjacent GC pairs followed by one AT pair.

The availability of synthetic doxorubicin or daunorubicin analogues with good DNA affinity and poor cytotoxic properties (Arcamone, 1984; Arcamone & Penco, 1986) leads us to investigate in great detail the mechanism and the specificity of DNA binding in a series of anthracyclines, with the hope of finding possible clues to the structural determinants of therapeutic effect. This investigation will include both thermodynamic and kinetic aspects. Here we report a kinetic analysis of the association and dissociation reaction of calf thymus DNA with five anthracyclines, whose structure, DNA affinity, and cytotoxicity for HeLa cells are summarized in Table I. Besides **1** and **2**, three other slightly modified anthracycline structures were selected so as to include strong (**2**) and weak (**5**) DNA binding drugs with similar cytotoxicity and analogues with similar DNA binding properties but widely different cytotoxicity (cf. **2**–**4**). Our approach here is to use fluorescence detection with stopped-flow kinetics, thus increasing the nucleotide/drug ratio up to values where site exclusion effects are not relevant. An extra bonus is obtained by working at low anthracycline concentration: exclusion of dimerization and other aggregation processes which may be significant even at concentrations as low as 10^{-5} M (Menozzi et al., 1984). The results confirm that anthracycline binding to DNA is a complex process requiring up to five steps for satisfactory data fitting.

Materials and Methods

The hydrochlorides of anthracycline **1**–**5** were obtained at Farmitalia C. Erba laboratories. Their purity was checked

0006-2960/89/0428-0274$01.50/0

Table I: Structure, DNA Binding, and Cytotoxic Properties of the Investigated Anthracyclines[a]

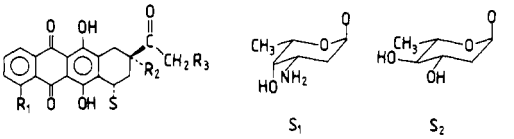

		R_1	R_2	R_3	S	n_{bp}	K_{DNA} (10^5 M^{-1})	ID_{50} (ng/mL)	reference
1	daunorubicin	OCH_3	OH	H	S_1	3.0	5.5	12.2	Arcamone, 1981
2	doxorubicin	OCH_3	OH	OH	S_1	3.2	24	14.9	Arcamone, 1981
3	4-demethoxydaunorubicin	H	OH	H	S_1	3.1	8.3	4.0	Arcamone, 1981
4	9-deoxydoxorubicin	OCH_3	H	OH	S_1	2.8	5.0	230	Arcamone & Penco, 1986
5	3′-desamino-3′-hydroxy-4′-epidoxorubicin	OCH_3	OH	OH	S_2	4.8	1.0	17.3	Cassinelli et al., 1985

[a] DNA binding constants, K_{DNA}, and site exclusion parameters, n_{bp} (see McGhee & von Hippel, 1974), were determined in TNE buffer at room temperature with the fluorescence quenching method according to a published procedure (Valentini et al., 1985). Standard deviations of both parameter estimates were less than 5% for compounds **1**–**3** but increased to about 10% in the case of anthracyclines **4** and **5**. The latter compounds show evidence of anomaly in the binding isotherms, which will be reported in a forthcoming paper (M. Menozzi, unpublished). Growth-inhibitory doses after 24 h of drug exposure, ID_{50}, are averages of several determinations on HeLa cells and differ slightly from those previously published.

by HPLC with a Waters μBondapak C_{18} column (3.9 × 300 nm, 10 μm) using as a mobile phase of 30% acetonitrile and 70% phosphate buffer (20 mM, pH 3). The sum of integrated contributions of extraneous peaks was always less than 5% of the total area. Stock solutions of the anthracyclines were prepared in water (**1**, **2**), in DMSO (**3**, **5**), or in the HPLC mobile phase (**4**) and then diluted with buffer up to the desired concentration. The concentration of the organic solvent in the final solution never exceeded 1%. Concentration of the stock solution was determined upon dilution with methanol containing 0.01 M HCl, on the basis of the following extinction coefficients: **1** (ϵ_{478} = 13 300 M^{-1} cm^{-1}); **2**, **4**, and **5** (ϵ_{478} = 13 600 M^{-1} cm^{-1}); **3** (ϵ_{482} = 11 600 M^{-1} cm^{-1}).

TNE buffer is composed of 0.05 M tris(hydroxymethyl)-aminomethane, 0.15 M NaCl, and 0.001 M EDTA, brought to pH 7 with HCl. Calf thymus DNA was a Sigma type I preparation. It was dissolved in TNE buffer with gentle magnetic stirring over several hours, then dialyzed twice against the same buffer, and finally filtered through a glass fiber filter of 1.2-μm pore size. Phage T7 DNA was a Sigma Ultrapure preparation. Concentration of DNA was estimated spectrophotometrically by using an extinction coefficient ϵ_{260} = 12 800 M^{-1} cm^{-1} per base pair unit. L-Ascorbic acid and sodium dodecyl sulfate (SDS) were Merck products. The sodium salt of 2,6-dichlorophenolindophenol (DCIP) was obtained from Fluka. All of the other chemicals and solvents were from Carlo Erba Divisione Analitica (Milano) and were of the highest purity available. Water purified through an HP 661A water purifier was used throughout.

Stopped Flow. Stopped-flow experiments were carried out with a Hi-Tech Scientific SF-51 apparatus in the fluorescence detection mode, using a 150-W Xenon lamp as light source. Excitation wavelength was set at a strong emission line of the lamp near 470 nm, in correspondence to a broad absorption region in the spectrum of the investigated anthracyclines. Fluorescence emission was collected through a glass cutoff filter (OG 530, provided by Hi-Tech) at right angles with excitation. Mixing syringes and reaction chamber were thermostated at 20.0 °C in both association and dissociation experiments. Equal volumes (75 μL) of a DNA solution and of an anthracycline solution were mixed in a typical association experiment. In a dissociation experiment a solution containing a preformed DNA-anthracycline complex was mixed with an equal volume of a 1.6% SDS solution. Data were collected on an Apple IIe computer by means of the Hi-Tech software package ADS-1, which provides a dual time base and a sampling rate of up to 50 μs/point. Instrument dead time τ_d and mixing rate constant k_{mix} were determined according to the procedure of Dickson and Margerum (1986) and found to be τ_d = 1.3 ± 0.1 ms and k_{mix} = 3000 ± 100 s^{-1} as an average of several determinations on the basis of amplitude measurements of the DCIP–ascorbic acid reaction at low pH (Hiromi, 1979). The reaction was followed with absorption detection and 10-mm optical path length, which provide observations of the entire reaction cell, as in the fluorescence mode. All observed rate constants k_{obsd} were then corrected according to the equation (Dickson & Margerum, 1986):

$$1/k = 1/k_{obsd} - 1/k_{mix} \quad (1)$$

Data Analysis. The time-dependent fluorescence signals deriving from two consecutive recordings with different sampling rate were combined, reduced to a total of 200 data points, and fitted with a sum of up to three exponentials by means of a computer program based on the algorithm ELORMA (Gampp et al., 1980) which was implemented to the ADS-1 package. The algorithm ELORMA separates linear parameters (amplitudes) from nonlinear ones (relaxation times), which are the only ones undergoing recursive optimization by means of a Marquardt procedure (Marquardt, 1963). The program has been tested with artificial data, simulating instrumental output under various conditions, and found to produce satisfactory analyses as long as consecutive relaxation times differed at least by a factor of 2–3. Amplitudes were corrected for an instrumental dead time of 1.3 ms. This provided an independent check of fitting completeness, by comparing the total corrected amplitude of the three kinetic steps versus the difference between the signal in the absence of DNA (free anthracycline) and that at equilibrium. The two quantities were found to be identical within experimental error, which was mostly due to inaccuracy in dead time determination.

Kinetic Models and Approximations. Site exclusion was taken into account with an approximation derived by Jovin and Stricker (1977) for relaxation kinetics (cf. eq A4). This approximation introduces an effective concentration c_{eff}, which can be computed from the known c_D, total drug concentration, and c_0, concentration of DNA base pairs, with values of the thermodynamic parameters K_{DNA} and n_{bp} as given in Table I. Equation A4 was found empirically to reproduce better the dependence of reciprocal relaxation times on c_D than eq A8, which was specifically derived for stopped-flow conditions. The analytical form of reciprocal relaxation times as functions of c_{eff} was computed by using the preequilibrium approximation (Bernasconi, 1976). Curve fitting to algebraic functions was performed with a nonlinear least-squares optimization routine

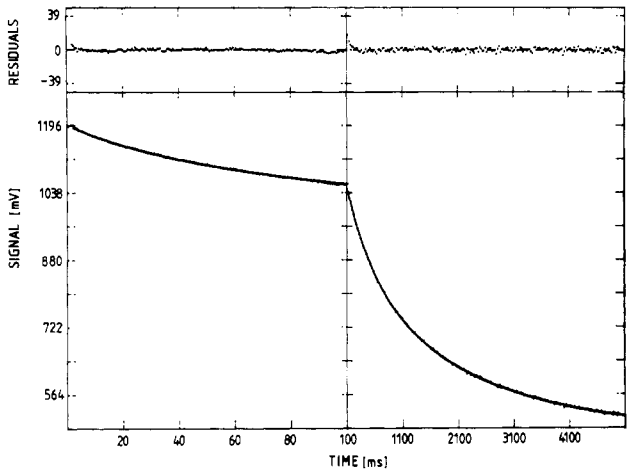

FIGURE 1: Time dependence of the fluorescence signal in a typical dissociation experiment carried out by mixing a preformed complex of doxorubicin (**2**, c = 1.6 μM) and calf thymus DNA [c = 100 μM (bp)] with a 1.6% SDS solution. The actual concentrations in the mixing chamber are half of the above. Data collection rate was 2 points/ms during the first 100 ms and 25 points/s in the next 5 s. Best fitting was obtained with the sum of the following three exponentials (solid line): A_0 = 477 mV, A_1 = 76 mV, A_2 = 244 mV, A_3 = 396 mV, $1/\tau_1$ = 28 s^{-1}, $1/\tau_2$ = 2.07 s^{-1}, and $1/\tau_3$ = 0.47 s^{-1}. Top panel shows the residuals.

Table II: Kinetic Parameters of SDS-Induced Dissociation of Anthracycline–DNA Complexes[a]

	$1/\tau_1$ (s^{-1})	A_1	$1/\tau_2$ (s^{-1})	A_2	$1/\tau_3$ (s^{-1})	A_3
1	28.5 ± 1	0.16	2.8 ± 0.1	0.42	0.72 ± 0.05	0.42
2	27.5 ± 0.5	0.12	2.1 ± 0.1	0.36	0.48 ± 0.03	0.52
3	26.8 ± 0.5	0.25	3.7 ± 0.1	0.62	0.65 ± 0.05	0.13
4	26.5 ± 1	0.26	3.4 ± 0.1	0.65	0.80 ± 0.1	0.09
5	38.0 ± 0.5	0.26	3.5 ± 0.1	0.42	1.2 ± 0.2	0.32

[a] Data are averages of at least three different measurements. After mixing, concentration of anthracyclines was 0.8 μM, SDS concentration was 0.8% (w/v), and DNA concentration varied from 50 to 100 μM (bp).

using the Marquardt method (Marquardt, 1963). In the matrix formalism, relaxation times were computed by numerically evaluating the roots of the characteristic equation of the corresponding 3 × 3 matrix at fixed values of c_{eff}. Parameter optimization was carried out by systematic variation starting from values obtained for the same set of experimental data with the preequilibrium approximation.

Results

Dissociation Kinetics. Figure 1 shows the time course of fluorescence signal in a typical dissociation experiment of the complex between **2** and calf thymus DNA mixed with 0.8% SDS in the stopped flow. The use of dual time basis illustrates the multiexponential nature of this reaction. Three exponentials are required to fit the data of Figure 1, as confirmed by the residuals of a two-exponential resolution being distinctly nonrandom [see Figure 1 in the supplementary material (see paragraph at end of paper regarding supplementary material)]. Increasing the number of exponentials did not improve the quality of fitting. Varying DNA concentration from 50 to 100 μM (bp) did not affect either relaxation times or relative amplitudes above experimental errors. Averaged results are collected in Table II as reciprocal relaxation times and relative amplitudes. Identical results were obtained for **1** and **2** with ultrapure T7 DNA in place of calf thymus DNA, thus excluding possible artifacts due to protein contaminants in the latter sample.

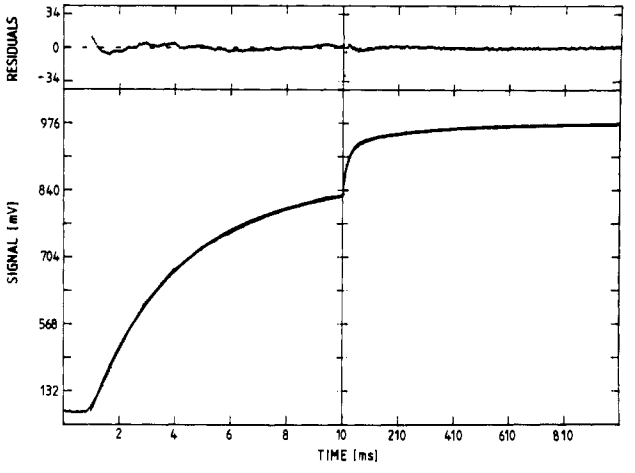

FIGURE 2: Time dependence of the fluorescence signal in a typical association reaction between doxorubicin (**2**, c = 0.8 μM) and calf thymus DNA [c = 48 μM (bp)]. Actual concentrations in the mixing chamber. Data were collected with a split time basis, at a rate of 20 points/ms in the first 10 ms and of 200 points/s in the next 1 s. The solid line is the best fitting sum of three exponentials (A_0 = 982 mV, A_1 = 409 mV, A_2 = 123 mV, A_3 = 45 mV, $1/\tau_1$ = 357 s^{-1}, $1/\tau_2$ = 47 s^{-1}, $1/\tau_3$ = 3.6 s^{-1}). The corresponding residuals are reported in the top panel of the figure.

Association Kinetics. Figure 2 shows an example of original data for the association reaction between **2** and calf thymus DNA. As in the case of dissociation, three exponentials are required to adequately fit the data. A resolution with only two exponentials is reported in Figure 2 of the supplementary material. Anthracycline concentration varied between 0.4 and 1.2 μM and that of DNA between 5 and 100 μM (bp). In the case of **5**, the maximal DNA concentration was increased up to 200 μM (bp). The ratio between DNA base pair and anthracycline concentration ranged from a minimum of 10 up to 250. A few experiments with T7 DNA gave results similar to those obtained with calf thymus DNA at equal base pair concentration. In agreement with the study of Chaires et al. (1985) on the interaction of **1** with DNA, the fastest reciprocal relaxation time was found to steadily increase with DNA concentration, while the other two reciprocal relaxation times reached a constant value with increasing DNA concentration. Dependence of reciprocal relaxation times on drug concentration at constant DNA concentration (50 μM) was investigated in the case of daunorubicin (**1**). A decrease of $1/\tau_1$ was observed with increasing drug concentration from 0.4 to 5 μM. This is in contrast with the increase predicted by eq A8. As is shown by Figure 3, eq A4 reasonably explains the observed changes in terms of c_{eff} variation. Similar results are obtained for the association reaction **2**–DNA. On the basis of this empirical observation, we have used c_{eff} throughout as the independent variable for the analysis of reciprocal relaxation times as functions of DNA concentration. The slight observed changes in $1/\tau_2$ were also accounted for by the change in c_{eff}. As expected, $1/\tau_3$ was practically unaffected by drug concentration changes in the above range.

Model Fitting to Association Data. The reciprocal relaxation times for the association reactions of anthracyclines **1**–**5** with calf thymus DNA are reported as functions of c_{eff} in Figures 4–8. The solid lines in the figures are curves obtained by fitting experimental data with the first four relaxations predicted by reaction mechanism III. One of the four computed relaxation times is assumed to correspond with an undetected phase having very low amplitude. Its dependence on c_{eff} is shown by a dashed line in the figures. The contribution of this hidden relaxation process was essential in describing

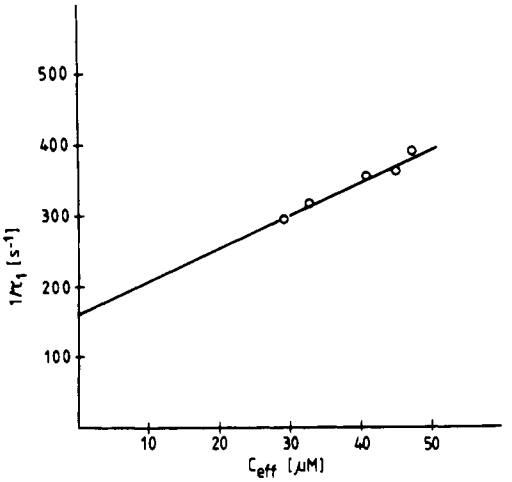

FIGURE 3: Variation of the fastest reciprocal relaxation time with changing total drug concentration in the association reaction between daunorubicin (**1**) and DNA. The DNA concentrations was kept constant (50 μM) and c_D varied between 0.4 and 5 μM. Data are reported as a function of c_{eff} (*decreasing* with increasing c_D) in order to compare with the linear dependence predicted by eq A4: $1/\tau = k_{on}c_{eff} + k_{off}$. The least-squares straight line produces values of these parameters ($k_{on} = 4.6 \times 10^6$ M^{-1}s^{-1} and $k_{off} = 159$ s^{-1}) that compare reasonably well with k_2 and k_{-2} as reported in Table III.

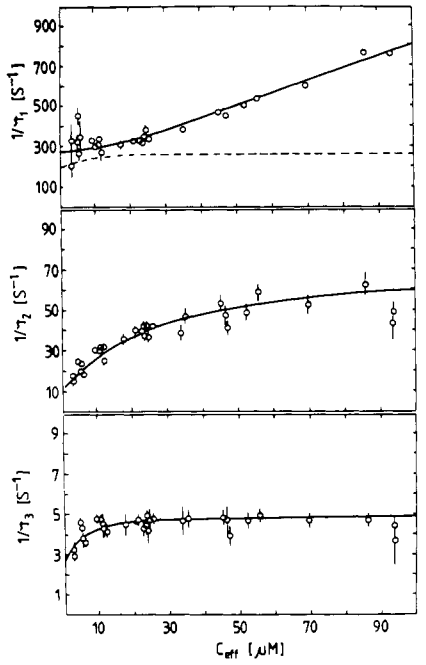

FIGURE 4: Dependence of the reciprocal relaxation times on c_{eff} for the association reaction between daunorubicin (**1**) and DNA. Best fitting curves have been computed with kinetic model III and a full matrix approach for the first two relaxation times. A dashed line shows the dependence on c_{eff} of the second eigenvalue predicted by the model. The dependence of $1/\tau_3$ on c_{eff} was fitted to eq 2 with a nonlinear regression procedure. All kinetic parameters are those reported in Table III.

the association reaction of **2** or **5** with DNA and improved the quality of data fitting in all other cases.

All kinetic parameters used to generate the fitting curves in Figures 4–8 are collected in Table III. Values of k_1, k_{-1}, k_2, k_{-2}, k_3, and k_{-3} were obtained by comparing the first two experimental relaxation times, respectively, to the largest and smallest eigenvalue of the kinetic matrix corresponding to the first three steps of mechanism III. A derivation of this matrix is included in the supplementary material. The hidden relaxation process was assigned to the intermediate eigenvalue.

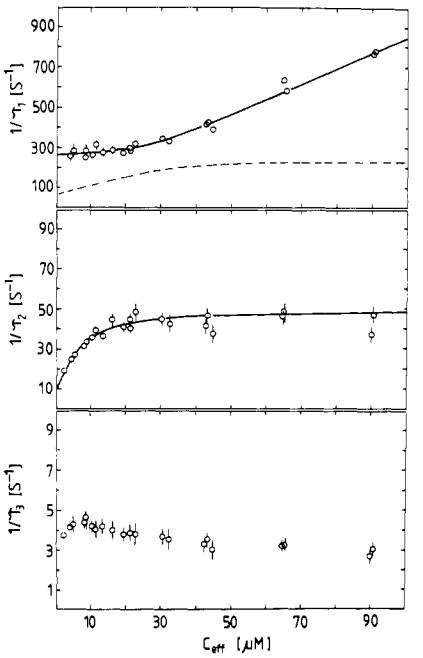

FIGURE 5: Dependence of the reciprocal relaxation times on c_{eff} for the association reaction between doxorubicin (**2**) and DNA. Best fitting curves as in Figure 4. Kinetic parameters are as reported in Table III. Data on $1/\tau_3$ could not be fit to any reasonable kinetic model and are though to be amplitude-weighted averages of two relaxations (see Discussion for details).

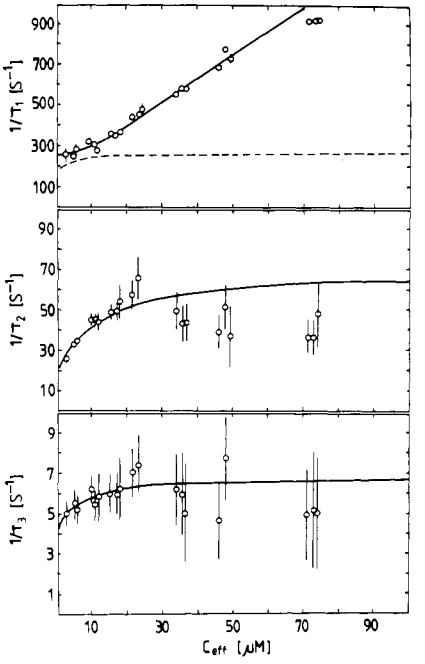

FIGURE 6: Dependence of the reciprocal relaxation times on c_{eff} for the association reaction between 4-demethoxydaunorubicin (**3**) and DNA. Best fitting curves as in Figure 4. Kinetic parameters are as reported in Table III.

The third experimental relaxation time was fitted with the analytical expression derived for step 4 after assuming preequilibrium of steps 1–3 in mechanism III:

$$1/\tau_4 = k_4 \frac{K_2K_3c_{eff}}{1 + (K_1 + K_2 + K_2K_3)c_{eff}} + k_{-4} \qquad (2)$$

where $K_i = k_i/k_{-i}$. In the course of parameter optimization with a nonlinear regression program, only k_4 and k_{-4} were actually used as variables and all of the equilibrium constants K_i were fixed to the values obtained from the analysis of the

Table III: Kinetic Parameters of the Anthracycline–DNA Association Reactions According to Mechanism III

	k_1 (M^{-1} s^{-1})	k_{-1} (s^{-1})	k_2 (M^{-1} s^{-1})	k_{-2} (s^{-1})	k_3 (s^{-1})	k_{-3} (s^{-1})	k_4 (s^{-1})	k_{-4} (s^{-1})	k_5 (s^{-1})	K_t (10^5 M^{-1})
1	0.5×10^6	270	6.0×10^6	140	60	15	3.2 ± 0.4	2.5 ± 0.2	0.9	6.1
2	0.8×10^6	260	7.0×10^6	30	30	20	(3)	(2.1)	(1)	18
3	0.9×10^6	260	11.0×10^6	130	45	27	4.9 ± 2.3	3.8 ± 1.0	0.2	4.5
4	0.8×10^6	230	9.2×10^6	130	55	23	4.3 ± 2.6	4.0 ± 1.2	0.1	4.5
5	0.8×10^6	330	1.8×10^6	90	28	18	4.5 ± 0.3	2.8 ± 0.1	1.4	1.4

[a] Rate constants k_1, k_{-1}, k_2, k_{-2}, k_3, and k_{-3} were estimated by fitting $1/\tau_1$ and $1/\tau_2$ data of association kinetics to the largest and smallest eigenvalue of the kinetic matrix corresponding to the first three steps of model III. Values of k_1 are the most inaccurate (a variation of ±30% could be tolerated by the accuracy of our data). The other parameters are estimated to be accurate within ±10%. Rate constants k_4 and k_{-4} were obtained by fitting eq 3 to $1/\tau_3$ data of association kinetics. Reported uncertainties are standar deviations as obtained from the nonlinear regression program. In the case of doxorubicin (**2**), k_{-4} was identified with $1/\tau_2$ of dissociation kinetics (see Table II) and k_4 was roughly estimated from the high c_{eff} limit of $1/\tau_3$ data of the association kinetics. Rate constants k_{-5} are assumed identical with $1/\tau_3$ values in dissociation experiments (Table II). Values of rate constant k_5 are guessed according to eq 4 from data of dissociation kinetics. The total binding constant K_t is computed according to model III: $K_t = K_1 + K_2[1 + K_3(1 + K_4 + K_5)]$.

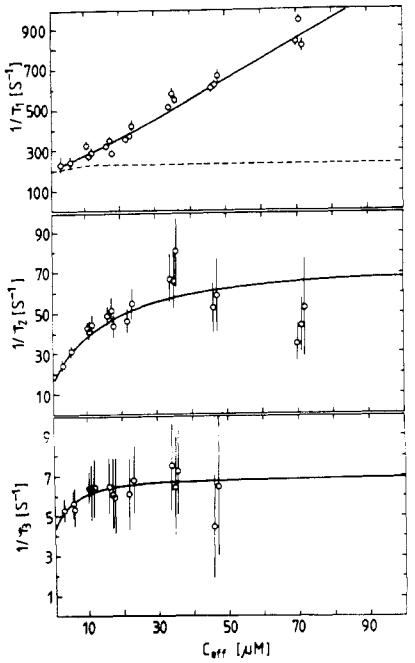

FIGURE 7: Dependence of the reciprocal relaxation times on c_{eff} for the association reaction between 9-deoxydoxorubicin (**4**) and DNA. Best fitting curves as in Figure 4. Kinetic parameters are as reported in Table III.

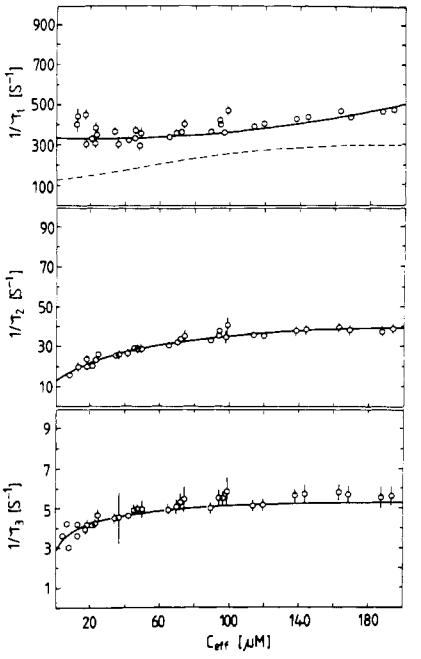

FIGURE 8: Dependence of the reciprocal relaxation times on c_{eff} for the association reaction between 3′-deamino-3′-hydroxy-4′-epi-doxorubicin (**5**) and DNA. Best fitting curves as in Figure 4. Kinetic parameters are as reported in Table III.

previous two steps. Data for the slowest relaxation process of the association reaction between doxorubicin (**2**) and DNA could not be fit to such an equation and were left uninterpreted (see Figure 5). A rationalization of this anomalous behavior is presented under Discussion. Rate constants of step 5 are roughly estimated from data of dissociation kinetics. Rate constant k_{-5} is identified with the slowest reciprocal relaxation time of dissociation kinetics (cf. $1/\tau_3$ in Table II). According to reaction mechanism III, the amplitudes of the two slow processes in the dissociation kinetics, A_2 and A_3, may be considered proportional to the relative amount of bound species B_4 and B_5 at equilibrium, thus relating the ratio of these two amplitudes with the ratio of equilibrium constants K_4 and K_5. Values of rate constant k_5 may then be derived from

$$k_5 = k_{-5}\frac{k_4 A_3}{k_{-4} A_2} \qquad (3)$$

Discussion

Site Exclusion. By use of fluorescence detection the association reaction between several anthracyclines and calf thymus DNA has been investigated at nucleotide/drug ratios extending up to a few hundreds. Under these conditions site exclusion effects become negligible and persistence of multiexponential kinetics is then a firm evidence of complexity in the association mechanism. However, reliable determination of dissociation rate constants required measurements down to as low as possible values of c_0. We never exceeded a ratio c_D/c_0 of 1/10, but a dependence of experimental rate constants on c_D is clearly observed under such conditions (see Figure 3). Equation A4, which was originally derived for relaxation experiments, reproduces this dependence better than eq A8, which is more pertinent to stopped-flow experiments. This observation is puzzling and remains unexplained, and we can only speculate why site exclusion appears to be fully developed at the level of the observable bimolecular step. We notice, however, that under our experimental conditions plots of reciprocal relaxation times vs c_{eff} or c_0 lead to similar results. Nevertheless, we have applied throughout the correction given by eq A4 on the basis of our empirical observation, and for better comparison with the work by Chaires et al. (1985), where the same correction has been used in interpreting stopped-flow experiments.

Kinetic Mechanism. The two limiting mechanisms proposed by Chaires et al. (1985) for daunorubicin–DNA interaction correspond to models I (three sequential steps) and II (three steps with branching) in Scheme I. The dependence of the three reciprocal relaxation times on c_{eff}, as obtained with preequilibrium conditions, is reported by Chaires et al. for

Scheme I

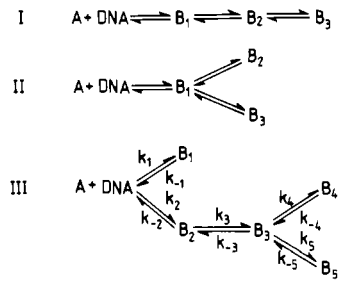

mechanism I. For convenience of the reader, we have collected in Table I of the supplementary material their analytical expressions and those similarly obtained for mechanism II and for the first three steps of mechanism III (vide infra). As can be easily verified, the dependence of relaxation times on c_{eff} is algebraically equivalent for the three mechanisms, which cannot be distinguished on this basis only. Correspondence of sequential and branched mechanisms has been discussed in more detail by Corin and Jovin (1986). Results of an analysis using the expressions of the first two relaxations in model I or II have been already reported for the association reaction of anthracyclines **1–4** with calf thymus DNA (Rizzo et al., 1988). The quality of fitting was satisfactory only for the case of **1** and perhaps **4**, while all other anthracyclines showed clear evidence of $1/\tau_2$ saturation at values of c_{eff} much lower than could be predicted by a model consistent with $1/\tau_1$ data. Specifically, the discrepancy was assigned to the value of the equilibrium constant computed from rate constants of the first, bimolecular step, being lower than required to describe relaxation data pertinent to the next step. Furthermore, total binding constants derived from three-step model analysis, K_t, compared poorly with experimental K_{DNA} values (Table I), these latter being always larger. In the case of **2**, the difference amounted to more than a factor of 10.

Inadequacy of three-step mechanisms is not a consequence of approximations or assumptions made in the derivation of a functional dependence for $1/\tau_i$ on c_{eff}. The analysis with a more accurate full matrix representation of the kinetic equations using any of the possible three-step kinetic models (from fully sequential to fully parallel) afforded a comparable poor fitting of experimental data. Experimental evidence then suggests that an appropriate kinetic model of DNA–anthracycline interaction must contain more than three steps, although three exponentials appear to be sufficient to fit both association and dissociation data. We find empirically that a five-step mechanism is necessary for a complete interpretation of both association and dissociation kinetics. These are best described by mechanism III in Scheme I, though alternative mechanisms cannot be definitely ruled out.

One step either concomitant to or immediately following the bimolecular one must be introduced in order to explain the apparent discrepancy described above for the analysis with three-step models. Both choices are in principle possible, but a branched mechanism offers an intuitive explanation to the apparent undetectability of one relaxation process, when the relaxation spectrum is analyzed in terms of normal modes of reaction [see Chapter 7 of Bernasconi (1976)]. In a simple mechanism comprising two parallel association steps (cf. steps 1 and 2 of mechanism III), one of the normal modes describes direct transfer between the two alternative reaction products B_1 and B_2. The amplitude of this normal mode strongly depends on the relative fluorescence of B_1 and B_2. The more similar are the two fluorescent yields, the lower is the amplitude. In fact, mechanism III provides an excellent interpretation of the first two experimental relaxation times as functions of c_{eff} in all five investigated cases (cf. Figures 4–8). Numerical simulation shows that the amplitude of predicted intermediate relaxation (dashed curves in these figures) is negligible when B_1 and B_2 have comparable fluorescent yields, both above 50% of that of the free drug.

The presence of step 5 is suggested by a comparison of dissociation rate constants obtained from the analysis of dissociation reactions (Table III) and those measured directly in SDS-induced dissociation kinetics (Table II). Possibly the fastest dissociation rate constant of Table II is an averaged contribution from steps 1–3 in the association mechanism. Of the two slow disociation rates in Table II, the faster one appears to have a counterpart in k_{-4} of Table III, but the slower one does not correspond with any measurable component of the association reaction. Most probably its contribution to the association reaction is too low for detection or the two expected relaxation processes are too close to be resolved by our data analysis. Evidence in favor of this latter hypothesis can be found in c_{eff} dependence of $1/\tau_3$ for doxorubicin (**2**)–DNA association (Figure 5). The presence of a maximum at $c_{eff} \approx 10\ \mu M$ and subsequent decrease of $1/\tau_3$ with increasing c_{eff} are not consistent with any acceptable kinetic mechanism and strongly indicate that such data are amplitude-weighted averages of two relaxation processes. A parallel rather than sequential arrangement of steps 4 and 5 is preferred because it explains the low amplitude of the slowest process by a mechanism similar to that invoked for steps 1 and 2 and it facilitates estimating the parameters of step 5 (see Results).

The extended mechanism III is also in very reasonable agreement with thermodynamic data, as can be verified in a comparison between values of the experimental binding constant K_{DNA} (see Table I) and the calculated one K_t (Table III). In the worst case (the association of **3** with DNA), the computed binding constant is 1.8 times lower than that determined in equilibrium experiments. This factor is within the uncertainty arising from determination of rate constants and crude estimation of the slower step parameters.

Comparison with Previous Work. Use of dual time basis and improved data analysis are probably responsible for detection of three exponentials in SDS-induced dissociation kinetics of **1** and **2**, where previous studies have reported a maximum of two exponential components (Fox et al., 1985; Chaires et al., 1985; Krishnamoorthy et al., 1986). Results on the association reaction of daunorubicin (**1**) with calf thymus DNA are in agreement with stopped-flow measurements based on absorption detection (Chaires et al., 1985). In spite of increased complexity, the qualitative picture of the association mechanism agrees with the conclusion by Chaires et al. that all steps but the bimolecular ones represent either conformational rearrangement of the drug/DNA complex or redistribution of bound drug to preferred sites without dissociation. Perhaps the major difference in our kinetic mechanism is the proposed competitive bimolecular association step which is assigned to the formation of a weak, probably nonintercalative complex. The rate constant of the bimolecular step leading to intercalation, k_2, is significantly higher in our study. Significant differences are also observed for other rate constants: the on-rate and off-rate assigned by Chaires et al. to the slowest step differ by a factor of 4, while the equivalent ones in our analysis (step 4) are about equal. Notice however that data on this exponential term are the most difficult to extract, because of the low relative amplitude.

Values of k_2 are comparable to the bimolecular on-rate measured for simple intercalators, such as proflavin (Ramstein

et al., 1980; Corin & Jovin, 1986) or ethidium (Ryan & Crothers, 1984; Mcgregor et al., 1985; Wilson et al., 1985). Because such compounds do not have slow relaxation times in their DNA association kinetics, and the observable bimolecular step leads to intercalation, we may similarly extrapolate an intercalated structure of intermediate B_2. Two possible mechanisms have been formulated to describe the molecular processes involved in intercalation (Wilson et al., 1985; Mcgregor et al., 1987). In one case (model a) a slow conformational rearrangement of DNA produces the intercalative site and is followed by diffusion-controlled formation of the intercalated complex at this site. The alternative mechanism (model b) is composed of diffusion-controlled formation of an outside complex, followed by a slow intercalation step. Recent experimental evidence (Mcgregor et al., 1987), based on viscosity dependence of the relaxation time in ethidium–DNA association, favors the first mechanism. Our data do not discriminate between the above two mechanisms. However, as we shall see in the next section, correlation of k_2 with drug structure suggests that this rate constant is a result of a series of molecular events including a diffusion-controlled association and most probably intercalation. This hypothesis is in contrast with the postulated nature of the first detectable intermediate in DNA–anthracycline association as an externally bound, electrostatically stabilized complex (Chaires et al., 1985; Krishnamoorthy et al., 1986), though we agree on the importance of electrostatic effects for the formation of this intermediate.

Correlation with Chemical Structure and Cytotoxicity. A comparison of rate constants k_2 of **1** or **2** with that of the uncharged synthetic analogue **5** (Table III) reveals a significant role of electrostatic forces in the bimolecular step. In fact, this rate constant decreases three to four times as a consequence of removal of the charged amino group in the sugar moiety. This factor may be reasonably attributed to the influence of the nucleic acid electrostatic potential on the diffusion-controlled rate of formation of the intercalated complex (model a). Electrostatic attraction almost doubles diffusion-controlled association rates between oppositely charged univalent electrolytes with respect to those involving neutral molecules [see, for instance, Chapter 3.2.3 of Schwarz (1986)]. A comparatively higher factor may be expected in the association between a positively charged molecule and a polyanion. Alternatively, according to model b, the effect may be attributed to stabilization of the outside complex by electrostatic forces in the cases of **1** and **2**.

Electrostatic effects on dissociation constant k_{-2} seem more difficult to disclose from our data, because minor structural factors greatly influence this parameter (cf. **1** and **2**). Nevertheless, restricting ourselves to compounds **2** and **5**, which only differ at the level of the sugar moiety, comparable differences are observed in k_2 and k_{-2} values. Chemical structure of the aglycone also appears to influence k_2. Elimination of methoxy function at C4 (**3**) or of the hydroxy group at C9 (**4**) brings about an increase of this rate constant. According to intercalation models a and b, respectively, the latter observation may be interpreted as indicating the following: (a) decreased steric requirements for the formation of a suitable intercalation site on DNA; (b) reduced steric hindrance in the transformation of the outside complex into the intercalated form. Interestingly, rate constants of step 1, leading to the hypothetical nonintercalative complex B_1, appear to be rather insensitive to the investigated structural modifications. This suggests that only the invariant upper chromophoric portion (see Table I) is involved in this form of interaction with DNA. Kinetic analysis of the intercalation mechanism clearly assigns to stabilization of intermediate B_2 the DNA affinity difference between daunorubicin and doxorubicin (Table I). A 4-fold increase of K_{DNA} in the latter compound is precisely matched by a 4-fold decrease of k_{-2}. Notably, destabilization of B_2 occurs after removal of the C_9-OH function as in **4**. Correlation of other rate constants with structure is not obvious. It appears however that the same factors which stabilize B_2 slow down its transformation into B_3.

A comparison of cytotoxicity data in Table I with rate constants, as determined either with association (Table III) or with dissociation kinetics (Table II), shows that no unequivocal correlation exists between these two properties. In particular, loss of activity in **4** is not followed by a similar increase of the slowest dissociation rate. Moreover, the same kinetic mechanism seems to be applicable in this as in the other four cases, and the kinetic parameters of the two compounds with highest (**3**) and lowest (**4**) cytotoxicity closely resemble each other. Compounds **2** and **5** have DNA binding constants differing by more than 20-fold; however, the corresponding cytotoxiciity values are only modestly different. Limitedly to this case, values of the slowest dissociation rate (Table II) appear to be a better predictor of the biological property.

Our conclusion contrasts with a generally observed correlation between biological activity and off-rate of anthracycline–DNA complexes (Fox et al., 1985; Foerster & Stutter, 1984). Perhaps one reason for this discrepancy is that we have used growth inhibition toward eukaryotic cells rather than antibacterial activity or protein synthesis inhibition as a measure of pharmacological potency. Growth inhibition of eukaryotic cells is indeed the property that is most relevant to antitumor activity of anthracyclines. Possibly, the different biological activities reflect distinct molecular mechanisms, which may share DNA binding as a common step. Support for such an opinion comes from recent results (Straney & Crothers, 1987) suggesting that antitumor activity of daunorubicin is not a result of transcription inhibition, and from the postulated role of the nucleic enzyme topoisomerase II as a target of anthracycline antitumor activity (Tewey et al., 1984; Pommier et al., 1985). In conclusion, our data support a cytotoxic mechanism where DNA binding is just one in a series of molecular events. Slow dissociation of the DNA complex may favor the pharmacological efficiency of these drugs. However, structural elements not related to nonspecific DNA binding, such as the presence of OH group at C9, must be present for a complete manifestation of cytotoxic power in anthracyclines. The role of such functional groups in the complex biological mechanism leading to cellular growth inhibition is still unclear and should be elucidated with suitable biochemical experiments.

ACKNOWLEDGMENTS

We thank Professors F. Arcamone and A. Vigevani and Drs. S. Penco and L. Valentini for many helpful discussions. We gratefully acknowledge the generous cooperation of Dr. C. Geroni, who provided cytotoxicity data on the investigated anthracyclines. V. R. thanks Dr. L. Tamm of the Biozentrum of the University of Basle, Switzerland, for his valuable advice concerning the algorithm ELORMA. We also gratefully acknowledge the insightful comments of one reviewer on the effect of site exclusion in our data.

APPENDIX

Effect of Site Exclusion on Relaxation Times. For the sake of clarity, references will be made to a simple association mechanism:

$$A + DNA \underset{k_{off}}{\overset{k_{on}}{\rightleftharpoons}} B \quad (A1)$$

whose rate equation is given by

$$db/dt = k_{on}c_s a + k_{off}b \quad (A2)$$

where small letters indicate concentration of the corresponding chemical species and c_s is the concentration of potential DNA binding sites [for an exhaustive discussion, see McGhee and vonHippel (1974)]. Under pseudo-first-order conditions ($c_s \approx c_0 \gg c_D$), eq A2 may be linearized (Bernasconi, 1976) and then integrated to give

$$b(t) = \frac{k_{on}c_0c_D}{1/\tau}(1 - e^{-t/\tau}) \quad (A3)$$

$$1/\tau = k_{on}c_0 + k_{off}$$

The presence of site exclusion will not affect this result as long as pseudo-first-order conditions are strictly obeyed. At comparable c_0 and c_D values, a complex multiexponential relaxation spectrum is expected (Epstein, 1979; Foerster & Stutter, 1984). However, for limited deviations from pseudo-first-order conditions, an extension of eq A2 is obtained by introducing a suitable correction. This correction has been originally presented by Jovin and Striker (1977) for the case of relaxation kinetics and consists of a modification of the term $c_0 + c_f$, the sum of total DNA base pair concentration and free drug concentration, which is the independent variable in relaxation analysis:

$$1/\tau = k_{on}c_{eff} + k_{off}$$

$$c_{eff} = f(r)c_0 - f'(r)c_f \quad (A4)$$

wher $f(r) = c_s/c_0$ and $f'(r) = df(r)/dr$ are known functions of $r = b/c_0$, the ratio of bound drug per DNA sites, and therefore depend on the DNA binding constant K_{DNA} and on the site exclusion parameter n_{bp} (McGhee & von Hippel, 1974):

$$f(r) = \frac{(1 - n_{bp}r)^{n_{bp}}}{[1 - (n_{bp} - 1)r]^{n_{bp}-1}} \quad (A5)$$

The derivation by Jovin and Striker is adapted here to conditions typical of stopped-flow experiments ($r \approx 0$). Near the origin, $f(r)$ is about linear and $f'(r)$ can be approximated with its value at $r = 0$. Therefore, we may write

$$f(r) \approx f(0) + f'(0)r = 1 + (1 - 2n_{bp})b/c_0 \quad (A6)$$

and from the definition of $f(r)$:

$$c_s \approx c_0 + (1 - 2n_{bp})b \quad (A7)$$

This result is inserted into eq A2, which, upon neglecting quadratic terms in b, can be integrated, leading to the same form as that of eq A3, provided that

$$1/\tau = k_{on}[c_0 + (2n_{bp} - 1)c_D] + k_{off} \quad (A8)$$

This result is strictly valid for a simple bimolecular reaction such as that depicted by eq A1. Rate constants of processes such as site redistribution or conformational changes of preformed complexes should obey eq A4, provided that appropriate values of r are used. Dependence of relaxation times on c_D can be used to distinguish applicability of eq A4 or A8. In the first case a decrease of $1/\tau$ is expected with increasing c_D [this arises mostly from the $f(r)$ term in eq A4]. In the second case, an increase of $1/\tau$ with increasing c_D is expected.

Supplementary Material Available

A derivation of the kinetic matrix for a three-step model, a table containing analytical expressions for relaxation times of kinetic models I–III, and two figures showing resolution of kinetic data with two exponentials (5 pages). Ordering information is given on any current masthead page.

Registry No. **1**, 20830-81-3; **2**, 23214-92-8; **3**, 58957-92-9; **4**, 84519-42-6; **5**, 86286-92-2.

References

Arcamone, F. (1981) *Doxorubicin: Anticancer Antibiotics*, Academic, New York.

Arcamone, F. (1984) in *X-Ray Crystallography and Drug Action* (Horn, A. S., & De Ranter, C. J., Eds.) pp 367–388, Oxford University Press, London.

Arcamone, F., & Penco, S. (1987) in *Molecular Mechanism of Carcinogenic and Antitumor Activity* (Chagas, C., & Pullman, B., Eds.) pp 225–241, Pontificia Academia Scientiarum, Vatican City.

Bernasconi, C. F. (1976) *Relaxation Kinetics*, Chapter 3, Academic, New York.

Cassinelli, G., Ballabio, M., Arcamone, F., Casazza, A. M., & Podestà, A. (1985) *J. Antibiot. 38*, 856–867.

Chaires, J. B., Dattagupta, N., & Crothers, D. M. (1985) *Biochemistry 24*, 260–267.

Chaires, J. B., Fox, K. R., Herrera, J. E., Britt, M., & Waring, M. J. (1987) *Biochemistry 26*, 8227–8236.

Chen, K.-X., Gresh, N., & Pullman, B. (1985) *J. Biomol. Struct. Dyn. 3*, 445–466.

Corin, A. F., & Jovin, T. M. (1986) *Biochemistry 25*, 3995–4007.

Dickson, P. N., & Margerum, D. W. (1986) *Anal. Chem. 58*, 3153–3158.

Epstein, I. R. (1979) *Biopolymers 18*, 2037–2050.

Foerster, W., & Stutter, E. (1984) *J. Biol. Macromol. 6*, 114–124.

Fox, K. R., Brassett, C., & Waring, M. J. (1985) *Biochim. Biophys. Acta 840*, 383–392.

Fritzsche, H., & Berg, H. (1987) *Gazz. Chim. Ital. 117*, 331–352.

Gampp, H., Maeder, M., & Zuberbuehler, A. D. (1980) *Talanta 27*, 1037–1045.

Hiromi, K. (1979) *Kinetics of Fast Enzyme Reactions. Theory and Practice*, pp 99–102, Halsted, New York.

Jovin, T., & Striker, G. (1977) in *Chemical Relaxation in Molecular Biology* (Pecht, I., & Rigler, R., Eds.) pp 245–281, Springer-Verlag, New York.

Krishnamoorthy, C. R., Yen, S.-F., Smith, J. C., Lown, J. W., & Wilson, W. D. (1986) *Biochemistry 25*, 5933–5940.

Marquardt, D. W. (1963) *J. Soc. Ind. Appl. Math. 11*, 431–441.

McGhee, J. D., & von Hippel, P. H. (1974) *J. Mol. Biol. 86*, 469–489.

Mcgregor, R. B., Clegg, R. M., & Jovin, T. M. (1985) *Biochemistry 24*, 5503–5510.

Mcgregor, R. B., Jr., Clegg, R. M., & Jovin, T. M. (1987) *Biochemistry 26*, 4008–4016.

Menozzi, M., Valentini, L., Vannini, E., & Arcamone, F. (1984) *J. Pharm. Sci. 73*, 766–770.

Mueller, W., & Crothers, D. M. (1968) *J. Mol. Biol. 35*, 251–290.

Phillips, D. R., & Crothers, D. M. (1987) *Biochemistry 25*, 7355–7362.

Pommier, Y., Schwartz, R., Zwelling, L. A., & Kohn, K. W. (1985) *Biochemistry 24*, 6406–6410.

Ramstein, J., Ehrenberg, M., & Rigler, R. (1980) *Biochemistry 19*, 3938-3948.
Rizzo, V., Sacchi, N., & Valentini, L. (1988) *Biochem. Pharmacol. 37*, 1819-1820.
Schwarz, G. (1986) in *Investigations of Rates and Mechanisms of Reactions* (Bernasconi, C. F., Ed.) Vol. 6, 4/E, Part 2, pp 27-139, Wiley, New York.
Straney, D. C., & Crothers, D. M. (1987) *Biochemistry 26*, 1987-1995.
Sturm, J. (1982) *Biopolymers 21*, 1189-1206.
Tewey, K. M., Rowe, T. C., Yang, L., Halligan, B. D., & Liu, L. F. (1984) *Science (Washington, D.C.) 226*, 466-468.
Valentini, L., Nicolella, V., Vannini, E., Menozzi, M., Penco, S., & Arcamone, F. (1985) *Farmaco, Ed. Sci. 40*, 377-390.
Wang, A. H.-J., Ughetto, G., Quigley, G. J., & Rich, A. (1987) *Biochemistry 26*, 1152-1163.
Wilson, D. W., Krishnamoorthy, C. R., Wang, Y.-H., & Smith, J. C. (1985) *Biopolymers 24*, 1941-1961.

Dynamics of Bases in Hydrated $[d(CGCGAATTCGCG)]_2$†

Agustin Kintanar,‖ Wen-Chang Huang, Deborah C. Schindele,‡ David E. Wemmer,§ and Gary Drobny*
Department of Chemistry, University of Washington, Seattle, Washington 98195
Received June 20, 1988; Revised Manuscript Received August 11, 1988

ABSTRACT: Solid-state ^2H NMR spectroscopy has been used to investigate the dynamics of a DNA oligonucleotide with a defined sequence, $[d(CGCGAATTCGCG)]_2$, which contains the *Eco*RI binding site. Quadrupole echo line shapes and spin–lattice relaxation times were obtained as a function of hydration on two different deuteriated samples, both in the form of the Na salt. In one sample, the C8 protons of all purines in the self-complementary dodecamer were exchanged for deuterons. In the other sample, a specifically labeled thymidine (C6 deuteriated) was synthetically incorporated at the seventh position (counting 5′ to 3′) in the sequence. The general trends for both samples were quite similar. At all levels of hydration, the data reveal the presence of a rapid, small-amplitude libration of the bases ($\tau_c \leq 1$ ns, 6°–10° amplitude). At the higher hydration levels (80% relative humidity or higher), the results indicate the presence of a much slower motion ($\tau_c \sim 10$–100 μs), which at 80% relative humidity is of small amplitude (~5°) and at higher hydration levels may be of larger amplitude. There is no evidence for large-amplitude (greater than ±10°) motion on a nanosecond or faster time scale under any hydration condition. The ^2H NMR results were analyzed with a dynamical model which treats the oligonucleotide as a deformable filament and which can include collective torsional fluctuations. The slow motion observed at high hydration levels is attributed to the uniform twisting mode (of the entire helix). Evidently, the various torsional modes decay more slowly in the viscous hydrated solid sample than in solution. The higher order (collective) torsional modes are predicted to occur on a nanosecond time scale and can account for the significantly reduced T_1 value found at high hydration levels.

The view of DNA as a rigid, uniform double helix has changed dramatically in the last few years. The determination of X-ray crystal structures of several synthetic DNA oligomers (Wing et al., 1980; Drew et al., 1981; Wang et al., 1982; Shakked et al., 1981) reveals that while these molecules have overall geometries similar to those of the A and B forms of DNA previously characterized by fiber diffraction techniques (Arnott & Hukins, 1972), there is considerable sequence-dependent variability of the local structure (Dickerson & Drew, 1981; Dickerson, 1983). Studies utilizing two-dimensional NMR methods indicate that such sequence-dependent structural microvariability also exists in DNA oligonucleotides in solution (Nerdal et al., 1988). An intriguing prospect is that this phenomenon provides the molecular basis for the specificity of protein–DNA interactions. Therefore, it is important to determine how well-defined are these structures and what is the range of allowed deviations from the average structure. In other words, what are the dynamics of DNA molecules?

Fortunately, scientific inquiry has not lagged in this area, and a large variety of physicochemical techniques has been used to study the motion of DNA in solution and in the solid state. The single-crystal X-ray diffraction data have been analyzed with atomic isotropic thermal factors (Drew et al., 1981, 1982) and also an anisotropic segmental rigid-body model (Holbrook & Kim, 1984) to extract information about the amplitudes and in some cases the direction of motion of the various moieties in the B-form DNA dodecamer. However, a full understanding of DNA dynamics requires the knowledge of the *rate* of motion, which is not available from the X-ray diffraction studies.

Several optical techniques have been used to study high molecular weight DNA including electric dichroism (Ding et al., 1972) and depolarized dynamic light scattering (Schmitz & Schurr, 1973; Schurr, 1977). These studies reveal that such high molecular weight DNA molecules are quite flexible, possessing slow coil-deformation (Rouse–Zimm) modes as well as more rapid end-over-end persistence length rotations. The

† This work was supported by National Institutes of Health Grant GM 32681 to D.E.W. and G.D.
‖ Present address: Biochemistry and Biophysics Department, Iowa State University, Ames, IA 50011.
‡ Present address: Ultra Diagnostics Corp., Seattle, WA 98105.
§ Present address: Department of Chemistry, University of California, Berkeley, CA 94720.

0006-2960/89/0428-0282$01.50/0